Transient Networks in ABA Block Copolymer–Microemulsion Systems

Christian Quellet,* Hans-Friedrich Eicke, Gu Xu, and Yves Hauger

Institut für Physikalische Chemie der Universität Basel, Klingelbergstrasse 80, CH-4056 Basel, Switzerland

Received October 6, 1989; Revised Manuscript Received January 17, 1990

ABSTRACT: ABA block copolymers (with hydrophilic A-blocks (POE) and a hydrophobic B-block (PI) have been shown to induce gel formation in water-in-oil microemulsions.[1] Gelation is preceded by a pronounced change of the viscosity at low copolymer concentration. This change resembles the dilute-to-semidilute transition encountered in solutions of polymer chains in good solvents. It is attributed to the formation of a transient network interconnecting microemulsion droplets via the apolar B-blocks. The relaxation time of disentanglement of A-blocks and the droplets is about 10 ms at 298 K, i.e., on the order of the lifetime of the micellar aggregates.

1. Introduction

We observed recently that ABA block copolymers consisting of hydrophilic (A = poly(oxyethylene)) and hydrophobic (B = poly(isoprene)) moieties induce gel formation in water-in-oil microemulsions. The transparent and homogeneous gels obtained in this way have interesting properties. They respond elastically to stresses of short duration by emitting a characteristic hum in the (low) audio-frequency range and flow if submitted to a gravitational shearing stress over a long period of time. The latter observation is typical of polymeric networks with very weak cross-links between the chains. The occurrence of a sound with a frequency below 10 kHz can be attributed to slow propagating modes in a networklike structure with a very low elastic modulus.[2] An isotropic directional distribution of cross-links within the gel and a narrow distribution of collective motional relaxation times of the network are further prerequisites.

Incidentally, the systems just discussed differ principally from the so-called viscoelastic surfactant solutions where flexible cylindrical micelles of surfactants are formed.[3–5]

ABA block copolymers dissolve easily in water-in-oil microemulsions at room temperature and within a range of composition where the structure of the microemulsion can be described by well-defined nanometer-sized aqueous droplets which hydrate the hydrophilic blocks, while the hydrophobic blocks experience preferential interactions with the apolar dispersion medium (oil).

Electrical conductivity measurements at low copolymer concentrations have shown association between the block copolymer and the microemulsion droplets. The system was a mixture of water, AOT (i.e., Aerosol-OT, sodium bis(2-ethylhexyl) sulfosuccinate), and isooctane, i.e., a W/O microemulsion and POE–PI–POE block copolymers.[6] These investigations let us suppose that two types of copolymer–nanodroplet complexes can be formed depending on the ratio of the molecular weights of the A- and B-blocks. If the mass of the B-block is larger than those of the A-blocks ($M_A/M_B < 1$), the copolymer adopts a core–shell conformation and forms a pseudo core–shell nanodroplet–copolymer complex in the microemulsion (Figure 1d). Such copolymers do not induce gel formation. In the case $M_A/M_B > 1$, extended conformations of the block copolymer are anticipated which lead to the formation of dimeric nanodroplet–copolymer complexes (Figure 1c). These latter copolymers initiate gel formation of the system at higher polymer concentrations. Both complex structures yield quantitatively different slopes of the electrical conductivity versus polymer concentration. Gelation does not require formation of a water-continuous network through the system. Hence, the electrical conductivity of the gel is small ($\simeq 10^{-6}$ ohm^{-1} m^{-1}).

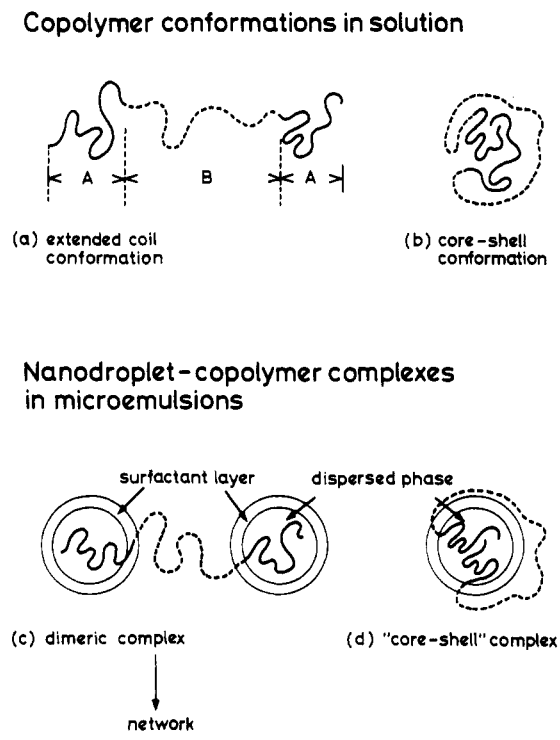

Figure 1. (a and b) Possible conformations of the triblock copolymer, ABA (A = hydrophilic block, B = hydrophobic block), and the corresponding aqueous nanodroplet–copolymer complexes. (c) Extended conformation and dimeric complex. (d) Core–shell complex, from ref 6.

All observations support the idea sketched in Figure 1, i.e., that the aqueous nanodroplets remain dispersed in the apolar medium while they are interlinked via the oil-compatible B-blocks.

In the present paper, we are concerned with a particular consequence of these copolymer–nanodroplet interactions, i.e., the pronounced break of the viscosity vs copol-

* Present address: 2, rue Jean-Sessler, CH-2502 Biel/Bienne, Switzerland.

0024-9297/90/2223-3347$02.50/0

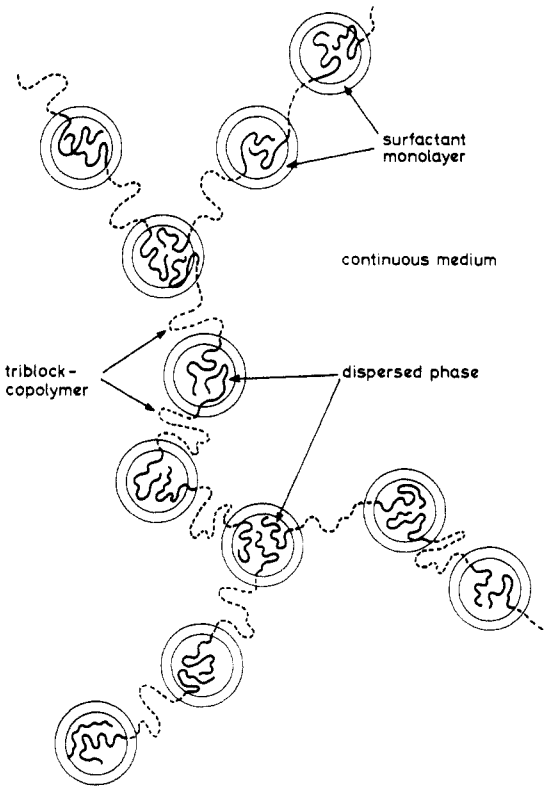

Figure 2. Possible structure of the transient network for $c_{copolymer} > c^*$.

ymer concentration plots (Figures 5 and 9). This occurs at low copolymer concentrations and at a temperature that is high with respect to the gel point. We suppose that the increase of viscosity is due to the formation of an entangled network of interconnected nanodroplets as depicted in Figure 2, for the description of which we refer to the transient network theory. According to this model, the entanglement points of the network are the nanodroplets that contain more than one POE-block. The distance between the entanglement points is controlled by the end-to-end distance of the PI-blocks.

2. Experimental Section

2.1. Chemicals. AOT (sodium bis(2-ethylhexyl) sulfosuccinate) from Fluka, Switzerland, was purified in an active carbon/MeOH slurry under stirring for about 24 h. The sample was filtrated and evaporated to dryness, and the residual water was removed under reduced pressure (3×10^{-3} Torr). Because AOT is hygroscopic, the purified surfactant was stored in a desiccator.

Isooctane (2,2,4-trimethylpentane) of highest grade obtained from Fluka was used without further treatment. Water was deionized and distilled twice.

The triblock copolymers (poly(isoprene-*b*-ethylene oxide), POE-*b*-PI-*b*-POE) have been synthesized and characterized at the Laboratoire de Chimie Macromoleculaire, ENSCM, Mulhouse (Prof. G. Riess), by G.X. The copolymers were prepared in THF by anionic polymerization. The polymerization technique was similar to that described in ref 7. Potassium naphthalide was used as initiator. The polymerization was carried out under argon at 203–223 K and terminated by adding a few drops of methanol. The resulting block copolymer was precipitated and washed with excess ether. The composition of the copolymer was determined by elementary analysis and NMR spectroscopy. Both methods yielded reasonably coinciding results. Molecular weights and their distributions have been determined by gel permeation chromatography (see Table I).

2.2. Preparation of Copolymer Solutions in the W/O Microemulsion. Known weighed-in amounts of triblock copolymers were dissolved in a W/O microemulsion at room temperature. This solution was stirred for 3–4 days with a magnetic stirrer until the initially turbid solutions became clear. The concentration of aqueous nanodroplets in the microemulsion is about 10^{20} droplets/dm^3.

Table I
Molecular Weights and Composition of Block Copolymers

	block copolymers				
	Cop-1	Cop-2	Cop-3	Cop-4	Cop-5
$\bar{M}_n^{POE}$	1740	13 500	22 000	6 500	13 050
$\bar{M}_n^{PI}$	85 260	61 500	39 000	19 500	15 950
POE/PI (w/w)	2/98	18/82	36/64	25/75	45/55
$\bar{M}_n^{COP}$	87 000	75 000	61 000	26 000	29 000
$\bar{M}_w^{COP}$	119 000	108 000	71 800	31 200	33 000
$\bar{M}_w/\bar{M}_n$	1.37	1.44	1.18	1.20	1.14
radius of gyration of PI, Å	105	89	71	50	45

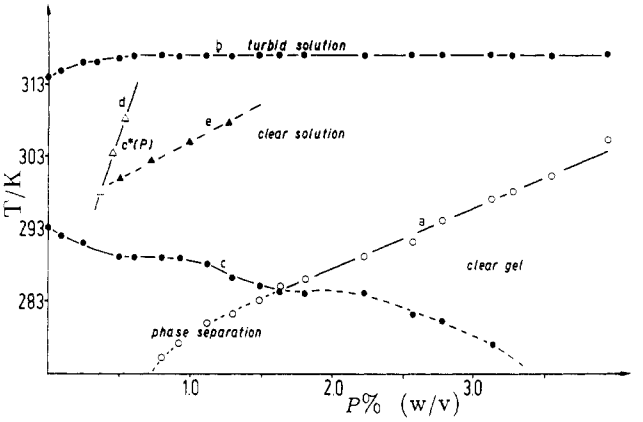

Figure 3. Section of a typical phase diagram of a gel-inducing copolymer containing microemulsion (Cop-3, see Table I). $w_0 = 60$, $c_{AOT} = 0.1$ mol dm^{-3}, c^* = copolymer concentration where crossing-over of the viscosity occurs (see text).

2.3. Measurements. Kinematic and (via the density) steady-state shear viscosity data were obtained with an automatic Ubbelohde viscometer, Vicomatic MS (Fica, France) equipped with thermostated capillaries.

The absence of a remarkable shear rate dependence of the viscosity was confirmed qualitatively by measurements with different capillary diameters and by using a PAAR modified falling ball microviscometer allowing continuous variation of the shear rate. Samples with the highest copolymer concentrations showed a slight shear rate dependence of viscosity, which was negligible as compared with the copolymer concentration dependence.

Light-scattering experiments were carried out using a light-scattering photometer (Sofica) with thermostated scattering cells. Sols were filtered directly into the scattering cell, using Millipore Millex-HV and Millex-GV filters with 0.5-μm pore size. The samples were then allowed to equilibrate for a definite time (1 day to 1 week) at the measuring temperature prior to any scattering experiment. In all cases, the scattering intensity was measured as a function of the scattering angle. The wavelength of the incident light was 546 nm.

3. Results and Discussion

A section of a typical phase diagram of a gel-inducing copolymer (Cop-3; 36 % POE, 64 % PI) in a particular W/O microemulsion is shown in Figure 3. The samples used to construct this diagram were transparent and homogeneous at room temperature. They underwent clear-to-turbid transitions at lower and higher temperatures (lines b and c in Figure 3). Demixing processes are similar to those observed at the cloud and haze points of the microemulsion without copolymer. The lower demixing temperature decreases with increasing copolymer concentration, while the upper demixing temperature depends only slightly on copolymer concentration. The observed con-

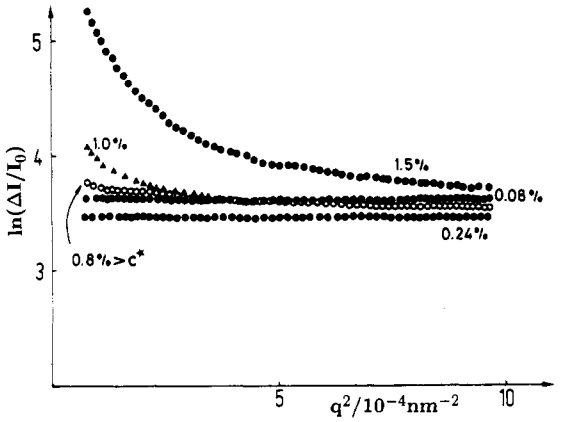

Figure 4. Guinier plots of light-scattering data for Cop-3. Parameter: copolymer concentration. T = 298 K, c_{AOT} = 0.1 mol dm^{-3}, w_0 = 60.

stancy of the upper demixing temperature with respect to copolymer concentration is due to the fact that the POE-blocks are expelled more and more from the aqueous phase of the droplets as the demixing temperature is approached. This conforms to the fact that poly(oxyethylene) becomes more hydrophobic with increasing temperature as apparent from the higher consolute temperature of aqueous solution of this polymer.[8]

The sol–gel transition is smooth and, hence, difficult to locate precisely. The gel point has been measured using the dropping ball method,[9] and, therefore, line a in Figure 3 is only qualitatively correct.

Line d in the low-concentration region of the phase diagram denotes the crossing-over between the smooth and the steep slopes of the viscosity plots versus concentration (Figure 5) at different temperatures, where we suppose that a network of interconnected nanodroplets via the hydrophobic B-blocks appears. The crossing-over concentration c^* depends very weakly on the temperature and on the composition of the copolymer. The length of the PI-block is not the controlling parameter regarding the appearance of an entangled network. The distance between the interconnected droplets must decrease for short PI-blocks, i.e., some segregation must occur, which, consequently, yields a larger mesh size of the network. The onset of network formation seems, however, to depend on the number of POE-blocks per nanodroplet. This is apparent from a comparison of c^* values for copolymers of different molecular weights (i.e., $c^* \simeq 0.4\%$ (w/v) for Cop-3 ($M_w \simeq 72\,000$) and 0.2% (w/v) for Cop-4 and Cop-5 ($M_w \simeq 32\,000$)) keeping the number of nanodroplets constant. The latter can reasonably be calculated from the average size of the droplets measured by light scattering, because of their moderate polydispersity (<20% in size). Calculation of the number of POE-blocks per nanodroplet is, however, difficult due to the high molecular weight polydispersity of the copolymer samples. A crude evaluation, based on the weight-average molecular weight of the copolymer, gives an average ratio of two A-blocks per nanodroplet at c^*. Increasing the number of nanodroplets causes c^* to shift toward higher copolymer concentration so that the above ratio is kept constant.

We now discuss qualitatively the scattering properties of the system above and below c^*. Guinier's plots of light-scattering data are shown in Figure 4 for the gel-inducing copolymer Cop-3. The curves show a weak dependence of the scattering intensity on the scattering angle q ($q = [2\pi/\lambda] \sin(\theta/2)$ with λ = wavelength of the incident light in the solution and θ = scattering angle) at low copolymer concentrations ($C_{Cop} \simeq 0.1$–0.4%). From $\Delta I/I_0$, the normalized intensity of the scattered light, we obtain the apparent average radii of gyration of the polymer–nanodroplet complexes ($R_{g,0}$):[10]

$$\Delta I/I_0 \propto \exp\{-(1/3)\langle R_{g,0}\rangle^2 q^2\}$$

Average radii of gyration between 10 and 15 nm are calculated on the basis of a large number of measurements. These radii correspond reasonably well to the estimated sizes of individual polymer-containing nanodroplets. Extended nanodroplet–polymer complexes may be difficult to differentiate from uncorrelated scatterers because the refractive index of the PI-blocks is similar to that of isooctane and the main contribution to scattering stems from the nanodroplets.

Formation of larger aggregates does not occur apparently in the low concentration region.

A similar scattering curve is observed at concentrations above the crossing-over concentration ($c_{Cop} \simeq 0.4$–1.0%). The scattering diagrams are typical of a nearly isotropic distribution of scattering centers, which would correspond to the intuitive model network postulated in Figure 2. This polymer seems, therefore, to adopt the ideal configuration of a network with a rather isotropic spatial distribution of junctions in water-in-oil microemulsions, at least at moderate copolymer concentrations $c^* < c \ll c_{gel}$. Such a network can be considered perfectly "calibrated" according to the definition of de Gennes.[11] It also conforms surprisingly well to a hypothetical model put forward by Burchard et al.[12]

The small deviation from Guinier's law in the low q-region stems from the formation of a few larger aggregates originating from some flocculation of nanodroplets. The curvature of the Guinier plots becomes more pronounced at higher polymer concentrations. In any case the radius of gyration of the single copolymer containing nanodroplet may be calculated from the limiting slope of the Guinier plots at high q-values.

Plots of the relative viscosity ($\eta_r = \eta/\eta_0$) against copolymer concentration for copolymers with various compositions (see Table I) are shown in Figure 5 at a constant number of nanodroplets. Block copolymers with shorter POE-blocks and longer PI-blocks (Cop-1 and Cop-2) show a monotonous increase of the viscosity within the whole concentration range. This agrees with the postulated "core–shell" structure b in Figure 1.

Gel-inducing copolymers with short PI-blocks and large POE/PI mass ratios show the pronounced break of the $\eta_r(c)$ plots discussed above, which we attribute to the occurrence of entanglement.

The different initial slopes of the viscosity curves seem to confirm the view addressed in ref 6 and are supported by electrical conductivity measurements that two kinds of copolymer–nanodroplet complexes are formed at low polymer concentration, depending on the copolymer conformation.

A general relation between the relative viscosity and the structural parameters of the dispersed species is furnished by

$$\eta_r = \eta/\eta_0 = 1 + \mathcal{F}(\Phi)$$

where $\mathcal{F}(\Phi) = \nu\Phi$ is the shape factor and Φ the volume fraction of complexes. Einstein's law demands $\nu = 2.5$ for spherical complexes.[13] An extension of Einstein's law due to Kuhn[14] postulates $\mathcal{F}(\Phi) = \nu\Phi + (\Phi/8)(a/b)^2$ for drained prolate ellipsoids. The latter equation allows us to determine a/b the axial ratio of the ellipsoid. In order to apply Kuhn's model, one needs a relation between the

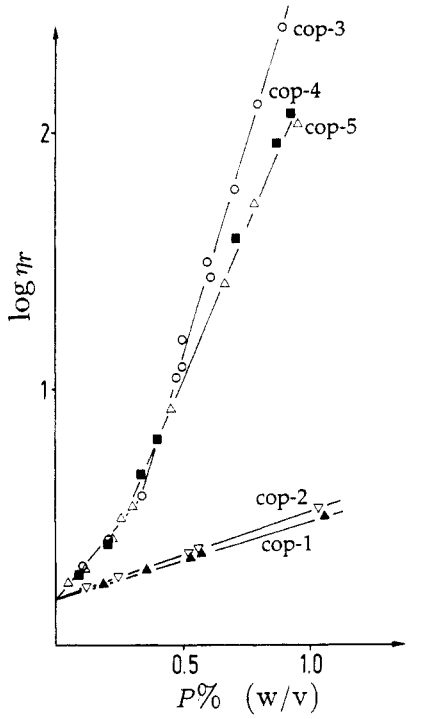

Figure 5. Semilog plots of the relative viscosity as a function of the polymer concentration for various copolymers (see Table I). T = 298 K, c_{AOT} = 0.1 mol dm^{-3}, w_0 = 60, from ref 6.

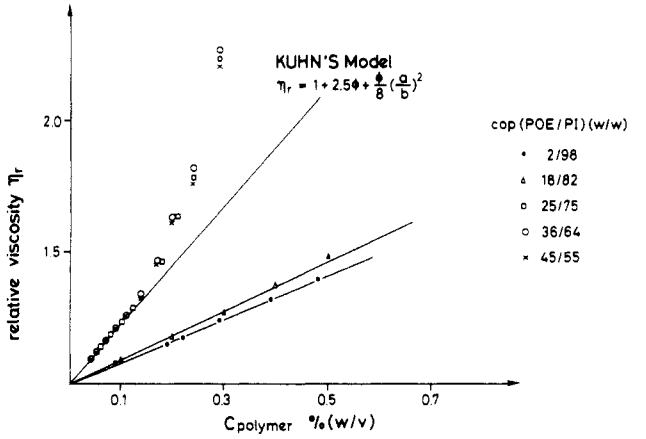

Figure 6. Plots of the relative viscosity versus copolymer concentration for various copolymers. Parameter: M_A/M_B. T = 298 K, c_{AOT} = 0.1 mol dm^{-3}, w_0 = 60. The full lines were calculated accordingly to Kuhn's and Einstein's equations (see text). a/b = axial ratio of the equivalent ellipsoid.

concentration of the copolymer (c) and $\Phi = N_{Av}cV_H/M$, where N_{Av}, M, and V_H are Avogadro's constant, the molecular weight, and the hydrodynamic volume of the complex, respectively. For Φ we assume (i) both, core–shell and dimeric, complexes to behave as rigid particles in the flow field and (ii) identical solvation of the PI-blocks in both complexes to be taken for granted. V_H is then obtained from the intrinsic viscosity of a system that consists of complexes having core–shell conformation, i.e.

$$[\eta] = \lim_{c \to 0} \frac{\eta_r}{c} = \nu \frac{N_{Av}V_H}{M} \qquad (1)$$

with ν = 2.5. The relation between the volume fraction of complexes and the copolymer concentration is found to be $\Phi = 32c_{Cop}$.

Semilogarithmic plots of the relative viscosity versus volume fraction, Φ, are shown in Figure 6. Core–shell complex forming copolymers Cop-1 and Cop-2 follow Einstein's law within the whole concentration range, while

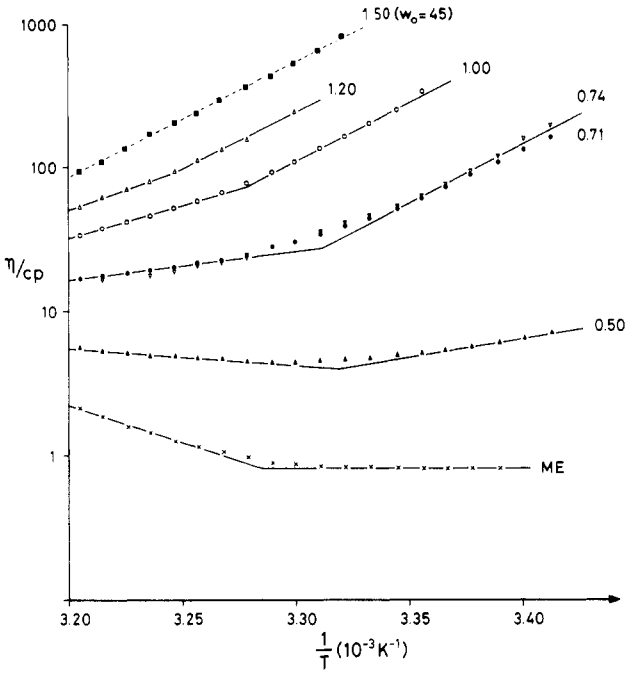

Figure 7. Arrhenius plots of the specific viscosity as a function of the reciprocal temperature for Cop-3. Parameter: copolymer concentration. c_{AOT} = 0.1 mol dm^{-3}, w_0 = 60. Dashed line: w_0 = 45.

copolymers Cop-3, Cop-4, and Cop-5 show steeper initial slopes. From these initial slopes we obtain the axial ratios a/b of the equivalent ellipsoids. The values are roughly between 5 and 6. This is in line with our idea that dimeric complexes are formed in the dilute region.

Arrhenius plots of the viscosity versus $1/T$ are shown in Figure 7. Measurements were made at temperatures between 292 and 312 K, i.e., where the system is transparent. The lower curve corresponds to the pure microemulsion. It shows a crossing-over at about 304 K, where the viscosity increases with increasing temperature. The crossing-over corresponds to the onset of the percolation, where swollen (fractal) clusters of nanodroplets are formed.[15] The observed activation energy of flow above the percolation temperature has no significance since the contribution of cluster formation dominates the temperature dependence of viscosity in these regions. Below the crossing-over temperature, the viscosity depends only slightly on the temperature as expected from a dispersion of weakly interacting droplets.

Addition of copolymer causes the viscosity to increase. The temperature dependence below and above the crossing-over temperature is also modified. Within the low-temperature region of the curves, a finite apparent activation energy of viscous flow (E^*) can be derived from the limiting slopes of the $\eta_r(1/T)$ plots.[16] This activation energy becomes independent of the polymer concentration, as apparent from the constancy of the slopes above c = 0.7%. The activation energy is 140 kJ/mol polymer.

Within the high-temperature region, the slope of the plots becomes positive at about 0.7% copolymer. The corresponding activation energy increases then with increasing polymer concentration to become equal to the low-temperature value (see the dotted line in Figure 7).

The existence of a crossing-over temperature which is associated with a change of E^* suggests that the network can break at moderate temperature if the copolymer concentration is too small. As apparent from the dotted line e in Figure 3, the location of the crossing-over is parallel to the sol–gel transition.

These results can be interpreted along with the postulated network structure in Figure 2. In order to derive the temperature dependence of the viscosity, we have recourse to the concept of the transient network introduced by Green and Tobolsky,[17] and Lodge.[18] In this model, the interactions between chains are described by localized junctions (see Figure 2) with finite lifetimes τ_R, which are shorter than the time scale of the observation. The concentration of junctions is $N(T,c,\tau_R)$, while the total concentration of junctions under steady-state conditions is $N_0(T,c)$. A steady state is reached under constant shearing stress where formation and dissociation of junctions occur at equal rates; i.e., $\langle dN_0(T,c)/dt \rangle = 0$.

Both rates are assumed to obey first-order kinetics; i.e.

$$dN_0(T,c)/dt = \pm k' N_0(T,c) \tag{2}$$

where k' is a rate (relaxation) constant. The number of junctions being formed (or destroyed) within the time interval dt is $\pm N_0(T,c)k'\,dt$.

Following, we consider the number of junctions that effectively contribute to the viscosity of the system. For this purpose we introduce the elastic modulus, which is, according to the classical theory of rubber elasticity, proportional to $N_0(T,c)$;[19] i.e.

$$G = aN_0(T,c)\,k_BT \tag{3}$$

where a is the average number of chain segments in the junctions (usually $a \sim 2$).

Applying a constant shearing stress $p_{2,1}$,[20] the shear $\gamma_{2,1}$ is given by

$$\gamma_{2,1} = \frac{1}{G}p_{2,1} = (aN_0(T,c)\,k_BT)^{-1}p_{2,1}$$

and the rate of shear, $\dot{\gamma}_{2,1}$, according to eq 2 is

$$\begin{aligned}\dot{\gamma}_{2,1} &= -p_{2,1}\frac{dN_0(T,c)}{dt}(aN_0^2(T,c)\,k_BT)^{-1} \\ &= p_{2,1}\frac{k'}{aN_0(T,c)\,k_BT} \\ &= p_{2,1}k'/G\end{aligned} \tag{4}$$

The ratio k'/G is the reciprocal viscosity coefficient, η; i.e.,

$$\eta = G/k' \tag{5}$$

The viscosity in the limit of low shearing stresses is, therefore, related to the rate constant characterizing the breaking and reforming of the transient junctions.

The temperature dependence of k' is taken to follow an Arrhenius relationship; i.e.

$$\begin{aligned}\eta(T) &= \frac{G}{k'_0}\exp\{E^*/k_BT\} \\ &= aN_0(T,c)\,k_BTk'_0{}^{-1}\exp\{E^*/k_BT\}\end{aligned} \tag{6}$$

where E^* is the activation energy of viscous flow, which does not depend on the chain concentration in the semidilute region, and $k'_0{}^{-1} = \lim\,(\eta/G)_{T^{-1}\to 0}$.

This equation may be compared to the generalized Maxwell equation for the steady-state shear viscosity of polymer chains above the overlapping concentration c^*; i.e.

$$\eta = G\tau_R \tag{7}$$

where G is the static (or "plateau") shear modulus and τ_R is the renewal time required by a polymer chain to escape from a given entangled situation. This renewal time turns out to be the inverse rate constant k'^{-1}:

$$\tau_R = k'_0{}^{-1}\exp\{E^*/k_BT\} \tag{8}$$

Hence, the renewal time may be obtained from a plot of the relative viscosity against $1/T$, provided $N_0(T,c)$ is known.

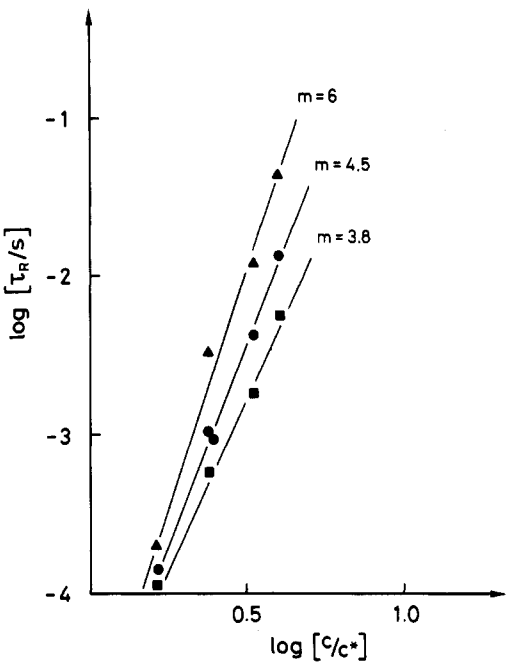

Figure 8. log–log plots of the renewal relaxation time versus copolymer concentration for the gel-inducing Cop-3 copolymer (see Table I): (▲) T = 293 K; (●) T = 298 K; (■) T = 302 K; c_{AOT} = 0.1 mol dm^{-3}, w_0 = 60.

Contrary to classical polymer–solvent systems, where $N_0(T,c)$ is usually difficult to evaluate, in the present case the number of chain segments in the junctions is directly related to the number of A-blocks located in the nanodroplets. If the temperature is not too close to the upper demixing temperature, this number is moreover nearly temperature independent. Our system offers, therefore, according to eqs 5 and 7, the possibility for calculating the renewal time of the chains in the network. Taking $N_0(T,c)$ and $aN_0(T,c)$ to be equal to the concentration of droplets and the concentration of A-blocks, respectively, i.e., neglecting loop formation, one obtains $\tau_R = k'_0{}^{-1}\exp\{E^*/k_BT\} \simeq 1$ ms at 298 K for $c_{Cop\text{-}3} = 0.7\%$. τ_R can be interpreted as the time required by the copolymer chain to escape from one microemulsion nanodroplet and penetrate into the other. Since τ_R is comparable to the lifetime of the unperturbated copolymer-free droplet, it is conceivable that the above motion is accompanied by a reorganization of the whole junction.

log–log plots of the renewal relaxation time, obtained from eq 7, versus c/c^* are shown in Figure 8. The relaxation time scales like $(c/c^*)^m$, where m is a nonuniversal exponent that depends, above $c = c^*$, on the temperature and the composition of the system.

Extrapolation to $c/c^* = 0$ yields $\tau_{R,0} = 15 \pm 5$ μs at 298 K, which may be compared with the rotational relaxation time of a single complex in the dilute region ($c \ll c^*$):[21]

$$\Theta_1 \cong 6\pi\eta_0V_H/k_BT \tag{9}$$

with V_H = hydrodynamic volume of the complex (eq 1) and η_0 = viscosity of the solvent. Equation 9 yields $\Theta_1 \simeq 40$ μs, which is slightly higher than $\tau_{R,0}$. The difference is probably due to the assumption of dumbbell-

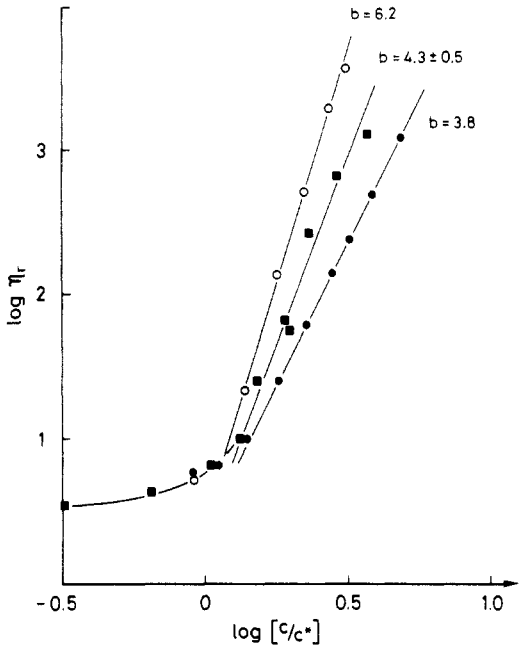

Figure 9. log–log plots of the relative viscosity versus copolymer concentration for the gel-inducing Cop-3 copolymer (see Table I): (○) T = 293 K; (■) T = 298 K; (●) T = 302 K; c_{AOT} = 0.1 mol dm^{-3}, w_0 = 60.

shaped rigid dimeric complexes, which overestimates V_H in eq 1.

log–log plots of the relative viscosity as a function of c/c^* for different temperatures are shown in Figure 9 for several temperatures. The viscosity exponent b is identical with m. Hence, we recover the concentration dependence of the elastic modulus $G \propto c/c^*$, which we have introduced in the calculation of τ_R. This confirms the self-consistency of the model of the transient network.

4. Conclusions

The solution behavior of ABA-block copolymer (hydrophile A-blocks and hydrophobic B-blocks) in microemulsions in the dilute and the semidilute regions has been investigated applying the concept of transient networks. The copolymers that can adopt an extended conformation in the microemulsion show a break of the viscosity plots vs copolymer concentration. We relate this phenomenon with the appearance of an entangled network of aqueous nanodroplets, which are interconnected via the B-blocks. The transient junctions of this network consist of microemulsion nanodroplets to which more than one A-block are attached.

These gel-inducing copolymers possess large ratios of the molecular weights of the A- and B-blocks (M_A/M_B < 1). The viscosity of dilute solutions of gel-inducing copolymers obeys Kuhn's law for drained ellipsoids. The axial ratio of the equivalent ellipsoid is between 5 and 6, which supports our view that dimeric complexes are present.

If $M_A/M_B > 1$, core–shell copolymer–nanodroplet complexes are formed, which do not form networks at high polymer concentrations. Also no crossing-over of the viscosity plots between dilute and semidilute regions is observed with these nongelling copolymers.

Above the crossing-over concentration c^* of gel-inducing copolymers, the viscosity scales like c^m, where m is not a universal exponent.

The flow behavior of the system is characterized by a typical activation energy of viscous flow on the order of 140 kJ/mol of copolymer. We expect this activation energy, which is constant at low temperature and high polymer concentration, to correspond to the energy required for shear-induced dissociation of junctions. The relaxation time associated with the dissociation of junction may be estimated. This "renewal time" (τ_R) ranges for Cop-3 at 298 K between 100 μs and 100 ms for copolymer concentrations between 0.3% and 1.5% (w/v) and $w_0 = [H_2O]/[AOT] = 60$. τ_R decreases continuously with increasing temperature.

It is therefore apparent that ABA-block copolymers form transient networks in water-in-oil microemulsions, provided the composition and conformation of the copolymer are matched in such a way that they fit the peculiar structure of the microemulsion. An important difference with respect to binary systems is the localization of the network junctions in the microemulsion droplets. The occurrence of such transient networks can account for the formation of gels with unusual properties at higher copolymer concentrations.

Acknowledgment. Financial support from the Swiss National Science Foundation (Project N19) is gratefully acknowledged.

References and Notes

(1) Eicke, H.-F.; Quellet, C; Xu, G. *Surf. Sci. Technol.* **1988**, *4*, 111.
(2) Bacri, J. C.; Dumas, J.; Levelut, A. *J. Phys. (Paris), Lett.* **1979**, *40*, L-231.
(3) Imae, T.; Abe, A.; Ikeda, S. *J. Phys. Chem.* **1988**, *92*, 1548.
(4) Hoffmann, H.; Rehage, H.; Platz, G.; Schorr, W. *Adv. Colloid Interface Sci.* **1982**, *17*, 275.
(5) Candau, S. J.; Hirsch, E.; Zana, R. *J. Phys. (Paris)* **1984**, *45*, 1263.
(6) Eicke, H.-F.; Quellet, C.; Xu, G. *Colloids Surf.* **1989**, *36*, 97.
(7) Marti, S.; Nervo, J.; Riess, G. *Prog. Colloid Polym. Sci.* **1975**, *58*, 114.
(8) Bailey, F. E.; Callard, R. W. *J. Appl. Polym. Sci.* **1959**, *1*, 56.
(9) Paul, D. R. *J. Appl. Polym. Sci.* **1967**, *11*, 439.
(10) Guinier, A.; Fournet, G. *Small-Angle Scattering of X-Rays*; John Wiley: New York, 1955. Huggins, M. B. *Light Scattering from Polymer Solution*; Academic Press: New York, 1972.
(11) de Gennes, P.-G. *Scaling Concepts in Polymer Physics*; Cornell University Press: Ithaca, NY, 1979.
(12) Burchard, W.; Bantle, S.; Mueller, M.; Reiner, A. *Pure Appl. Chem.* **1981**, *53*, 1519.
(13) Tanford, C. *Physical Chemistry of Macromolecules*; John Wiley: New York, 1961.
(14) Kuhn, W. *Z. Phys. Chem.* **1932**, *A161*, 1. Kuhn, W.; Kuhn, H. *Helv. Chim. Acta* **1945**, *28*, 97.
(15) Eicke, H.-F.; Hilfiker, R.; Thomas, H. *Chem. Phys. Lett.* **1986**, *120*, 272. *Ibid.* **1986**, *125*, 295. Hilfiker, R.; Eicke, H.-F. *J. Chem. Soc., Faraday Trans. 1* **1987**, *83*, 1621.
(16) Bueche, F.; Cashin, W. M.; Debye, P. *J. Chem. Phys.* **1952**, *20*, 1956.
(17) Green, M. G.; Tobolsky, A. T. *J. Chem. Phys.* **1946**, *14*, 80.
(18) Lodge, A. *Trans. Faraday Soc.* **1956**, *52*, 120.
(19) Dobson, G. R.; Gordon, M. *J. Chem. Phys.* **1965**, *43*, 705.
(20) The subscripts 1 and 2 refer to the direction of stress and shear, respectively.
(21) de Gennes, P.-G. *Macromolecules* **1976**, *9*, 594.